

Predicting Gibbs State Expectation Values with Pure Thermal Shadows

Luuk Coopmans,^{1,*} Yuta Kikuchi,² and Marcello Benedetti¹

¹Quantinuum, Partnership House, Carlisle Place, London SW1P 1BX, United Kingdom

²Quantinuum K.K., Otemachi Financial City Grand Cube 3F, 1-9-2 Otemachi, Chiyoda-ku, Tokyo, Japan
(Dated: June 10, 2022)

The preparation and computation of many properties of quantum Gibbs states are essential for algorithms such as quantum semi-definite programming and quantum Boltzmann machines. We propose a quantum algorithm that can predict M linear functions of an arbitrary Gibbs state with only $\mathcal{O}(\log M)$ experimental measurements. Our main insight is that for sufficiently large systems we do not need to prepare the n -qubit mixed Gibbs state explicitly, but instead we can evolve a random n -qubit pure state in imaginary time. The result then follows by constructing classical shadows of these random pure states. We propose a quantum circuit that implements this algorithm by using quantum signal processing for the imaginary time evolution. We verify the algorithm numerically by simulating the circuit for a 10 spin-1/2 XXZ-Heisenberg model.

Introduction – Gibbs states are mixed quantum states that describe quantum systems in thermodynamic equilibrium with their environment at finite temperature, and play a central role in quantum statistical mechanics [1]. Their properties are of importance for a wide range of applications [2], including the design of complex quantum materials in condensed matter physics and quantum chemistry, optimization with quantum semi-definite programming, and machine learning with quantum Boltzmann machines.

Preparing Gibbs states and computing Gibbs state expectation values are highly non-trivial tasks. Existing algorithms can have rather complicated implementations and may apply only to a limited set of systems. Classical algorithms suffer from the exponentially growing Hilbert space or have a sign problem for some Fermionic systems [3]. Fault-tolerant quantum algorithms have better asymptotic scaling [4, 5], but are limited by current hardware constraints and high levels of noise. Variational quantum algorithms can prepare Gibbs states [6, 7] and cope with some hardware limitations, but require many experimental measurements for each optimization step and may suffer from barren plateaus [8]. Other quantum approaches based on minimally entangled typical thermal states (METTS) [9, 10] set up a Markov chain that potentially has a long thermalization time.

Gibbs states can be represented mathematically by a density matrix of the form $\rho_\beta = e^{-\beta H}/Z$, where H is the system Hamiltonian, β is the inverse temperature, and $Z = \text{Tr} e^{-\beta H}$ is the partition function. In this Letter, we propose an efficient quantum algorithm to estimate a large number of Gibbs state expectation values without preparing and measuring the mixed state ρ_β . This is achieved by combining thermal *pure* quantum (TPQ) states [11–20] and classical shadow tomography [21–27]. One way to generate a thermal pure quantum state is by imaginary time evolution, $e^{-\beta H/2}|\phi\rangle$, of a n -qubit random state $|\phi\rangle$. We show that, if the probability distribution over the initial states, $|\phi\rangle$, forms at least a quantum 2-design [28], the imaginary time evolved states are able

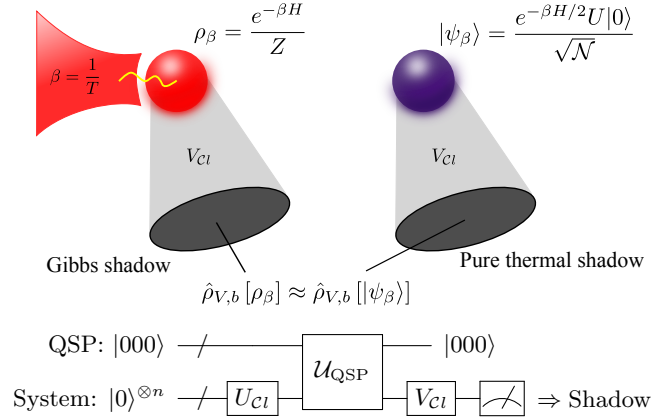


FIG. 1. Top: The classical shadows of a Gibbs state ρ_β , here represented as a quantum system (red sphere) in thermal equilibrium with its environment (red bath), are equal to the classical shadows constructed from a thermal pure quantum state $|\psi_\beta\rangle$ (purple sphere). The random measurement direction of the shadows is determined by the Clifford unitary V_{Cl} . Bottom: A circuit diagram of the quantum circuit that implements a pure thermal shadow with quantum signal processing (QSP).

to approximate the expectation values of ρ_β up to an error that falls off exponentially with the system size, n .

Classical shadow tomography is then exploited to construct an efficient classical representation of these TPQ states from outcomes of randomized measurements. Using the results from Ref. [23] we show that for sufficiently large systems we can estimate M Gibbs state expectation values using $\mathcal{O}(\log M)$ measurements of a single prepared TPQ state. This is remarkable because the required number of measurements is similar to the case where we had actually prepared the Gibbs state (e.g. via a purification using $2n$ qubits [5]).

We also propose a practical implementation of the algorithm. We begin by preparing the initial state using a polynomial-depth Clifford circuit. This suffices to produce a quantum 2-design. We then approximate the

imaginary time evolution using quantum signal processing (QSP) [29–32]. This approach is very general (i.e., it applies to any quantum Hamiltonian H , in principle), and offers great control since we can systematically trade off circuit depth for accuracy. For the randomized measurement, we use another Clifford circuit. The complete circuit comprising a Clifford circuit, a QSP circuit, and a randomized measurement, is shown in Fig. 1, and uses a total number of qubits linear in the system size, n . We numerically simulate this quantum circuit for a quantum system of 10 spin-1/2 particles in the XXZ-Heisenberg model [33, 34] to support our theoretical findings.

Thermal Pure Quantum States – A TPQ state is any pure state, $|\psi\rangle$, that is able to estimate a fixed set of properties (expectation values) of a sufficiently large mixed thermal state, specified by some specific statistical ensemble. For the thermodynamic (canonical) Gibbs ensemble, following Ref. [15], we define it to be any pure state $|\psi\rangle$, which is drawn at random, and that satisfies

$$\Pr[|\langle\psi|O_j|\psi\rangle - \text{Tr}\rho_\beta O_j| \geq \epsilon] \leq C_\epsilon e^{-\alpha n}, \quad (1)$$

for all O_j in some predefined set of Hermitian operators $\{O_j\}$. The constants C_ϵ and α will be specified later.

We now show that the pure states generated by imaginary time evolution,

$$|\psi_\beta\rangle = \frac{e^{-\beta H/2}U|0\rangle}{\sqrt{\langle 0|U^\dagger e^{-\beta H}U|0\rangle}} \equiv \frac{e^{-\beta H/2}U|0\rangle}{\sqrt{\mathcal{N}}}, \quad (2)$$

where $U \in \mathcal{Cl}(2^n)$ is a random unitary drawn from the n -qubit Clifford group, satisfy Eq. (1). These TPQ states are slightly different from the ones originally proposed in Ref. [15], and also differ from the ones used in Ref. [18] for classical numerical simulations. There, a particular form of Haar random states for $U|0\rangle$ is used, which on a quantum computer would require exponential circuit depth. Our choice of $U \in \mathcal{Cl}(2^n)$ yields a unitary 3-design [35] and thus it replicates Haar integrals up to the third moment. This has the advantage of requiring only $\mathcal{O}(n^2/\log n)$ quantum gates [36].

Firstly, as shown in detail in the Supplemental Material (SM), the expectation value of an arbitrary Hermitian operator O in the random pure states $|\psi_\beta\rangle$ is, on average,

$$\mathbb{E}_U[\langle\psi_\beta|O|\psi_\beta\rangle] \approx \text{Tr}\rho_\beta O + \text{Tr}\rho_\beta^2(\text{Tr}\rho_\beta O - \text{Tr}\rho_{2\beta} O). \quad (3)$$

Here \mathbb{E}_U denotes the ensemble average with respect to the n -qubit Clifford group $U \in \mathcal{Cl}(2^n)$.

A similar calculation for the variance of the expectation value with respect to U yields

$$\begin{aligned} \text{Var}[\langle\psi_\beta|O|\psi_\beta\rangle] &\approx \\ \text{Tr}\rho_\beta^2 &\left(\frac{\text{Tr}(Oe^{-\beta H})^2}{\text{Tr}e^{-2\beta H}} - 2\text{Tr}\rho_\beta O\text{Tr}\rho_{2\beta} O + (\text{Tr}\rho_\beta O)^2 \right). \end{aligned} \quad (4)$$

Both the bias in Eq. (3) and the variance in Eq. (4) are proportional to the purity of the Gibbs state, $\text{Tr}\rho_\beta^2$. Since the Gibbs state ρ_β minimizes the Helmholtz free energy, $F_\beta = -\log Z/\beta$, we can write

$$\text{Tr}\rho_\beta^2 = \frac{\text{Tr}e^{-2\beta H}}{Z^2} = e^{-2\beta(F_{2\beta}-F_\beta)} = \mathcal{O}(e^{-n}). \quad (5)$$

The last equality follows from properties of the free energy, i.e., the extensivity, $F_\beta \propto n$, [37] and the monotonicity with respect to the inverse temperature, $F_{2\beta} > F_\beta$. The terms that multiply the purity in Eqs. (3) and (4) have the form of expectation values and can be bounded by the spectral norm, $\|O\|^2$. This means that for operators with polynomially large $\|O\|^2$, the variance vanishes exponentially with n [38]. After application of Markov's inequality (see SM) we find that $|\psi\rangle = |\psi_\beta\rangle$ satisfies Eq. (1) with $C_\epsilon = 4\|O\|^2/\epsilon^2$ and $\alpha n = 2\beta(F_{2\beta}-F_\beta)$.

Hence, the expectation values with respect to the random pure states $|\psi_\beta\rangle$ can be used as estimators for Gibbs state expectation values of polynomially sized operators O , for a sufficiently large system and finite β . Importantly, for $\beta = \infty$, i.e., when the Gibbs state approaches the ground state of H , the Gibbs state becomes pure, $\text{Tr}\rho_\beta^2 = 1$, and the error remains finite for any system size n . For all other β , the rate of exponential decay, and thus how large n needs to be, is dictated by $F_{2\beta}-F_\beta$. The exact error, therefore, depends on which specific system Hamiltonian H one considers, the inverse temperature β , and also the spectral norm of the observable $\|O\|$. This means that in some specific instances [15, 18] using only a single TPQ state is sufficient (see SM). In contrast, approaches that do not have a vanishing variance, such as algorithms based on METTS [9, 10], may require multiple pure states.

Pure Thermal Shadows – Classical shadow tomography [21–23] is a method to efficiently predict many properties of a prepared quantum state, ρ , by performing randomized measurements and constructing efficient classical representations (shadows) from the measurement outcomes. In Ref. [23] it was proven that one can predict M properties of ρ from $\mathcal{O}(\log M)$ measurements (see SM for a review). For this reason, classical shadow tomography is particularly beneficial in scenarios where one needs to compute many observables, such as in variational quantum algorithms and quantum fidelity estimation [27].

To predict many properties of a Gibbs state ρ_β one can prepare a purification of ρ_β on $2n$ qubits and apply classical shadow tomography. Here, instead, we simplify the process by constructing shadows of the n -qubit TPQ states $|\psi_\beta\rangle$. We refer to these as *pure thermal shadows*. Notably, in the limit of large system size, the number of state preparations and measurements required for predicting M properties to a certain accuracy, becomes similar to the case where we prepare and measure ρ_β directly.

The first step of the algorithm is the application of a random unitary, V , to the TPQ states, $|\psi_\beta\rangle \mapsto V|\psi_\beta\rangle$.

The operation V can either be a random n -qubit Clifford unitary, $V \sim \text{Cl}(2^n)$, for a random Clifford measurement, or a tensor product of single qubit Clifford unitaries, $V \sim \text{Cl}(2)^{\otimes n}$, for a random Pauli measurement. Subsequently, a computational basis measurement of $V|\psi_\beta\rangle$ is performed to obtain a n -qubit bitstring outcome, $|b\rangle$. The thermal shadows,

$$\hat{\eta}_{V,b} = \mathcal{M}^{-1}(V^\dagger |b\rangle\langle b| V), \quad (6)$$

can be constructed with $\mathcal{M}^{-1}(X) = (2^n + 1)X - \mathbb{1}\text{Tr}X$. As V is a Clifford circuit, and $|b\rangle$ a bit string, the shadow can be constructed and stored classically efficiently.

By averaging over both the unitary V of the randomized measurements, and the unitary U of the TPQ states $|\psi_\beta\rangle$, we find that the expectation values of the pure thermal shadows satisfy

$$\mathbb{E}_U \mathbb{E}_{V,b} [\text{Tr} \hat{\eta}_{V,b} O] = \mathbb{E}_U [\text{Tr} |\psi_\beta\rangle\langle\psi_\beta| O]. \quad (7)$$

Here $\mathbb{E}_{V,b}$ includes both the classical average over the random circuits V as well as the quantum average of the measurement outcomes $|b\rangle$ via Born's probabilities. The expectation value of the shadow $\hat{\eta}_{V,b}$ is thus the same as the expectation value of $|\psi_\beta\rangle$. By Eqs. (3) and (5), this becomes equal to the Gibbs state expectation value, $\text{Tr} \rho_\beta O$, as we increase n .

The success probability of the algorithm depends on the mean-squared error, σ^2 , of the pure thermal shadow expectation value from the true Gibbs state expectation value. For random Clifford measurements, $V \sim \text{Cl}(2^n)$, we find (see SM) that this error evaluates to

$$\begin{aligned} \sigma^2 &= \mathbb{E}_U \mathbb{E}_{V,b} [(\text{Tr} \hat{\eta}_{V,b} O - \text{Tr} \rho_\beta O)^2] \\ &= \text{Tr} O_0^2 + 2\text{Tr} \rho_\beta O_0^2 - (\text{Tr} \rho_\beta O_0)^2 + \mathcal{O}(e^{-n}). \end{aligned} \quad (8)$$

Here, we have defined $O_0 = O - \mathbb{1}\text{Tr}O/2^n$ as the traceless part of the operator O . Similarly, for random Pauli measurements, $V \sim \text{Cl}(2)^{\otimes n}$, we obtain

$$\sigma^2 = 3^k - (\text{Tr} \rho_\beta O)^2 + \mathcal{O}(e^{-n}), \quad (9)$$

where O is now a k -local Pauli operator [39]

Remarkably, these mean-squared errors are, up to an exponentially small bias, the same as the σ^2 of shadows constructed from randomized Pauli and Clifford measurements of a prepared ρ_β (see SM). This means that constructing shadows of the TPQ state is as good as constructing shadows of the true Gibbs state.

In the scenario in which we wish to predict a total of M Gibbs state expectation values, we invoke a specific form of Theorem 1 in Ref. [23] for a median-of-means estimator. This gives the main result of this Letter, which can be summarized by the following theorem:

Theorem 1. *Given M Hermitian operators O_1, \dots, O_M , and accuracy parameters $\epsilon, \delta \in [0, 1]$. A total of*

$$n_{\text{shadows}} = NK = \frac{27 \log(M/\delta)}{\epsilon^2} \max_j [\sigma_j^2] \quad (10)$$

classical shadows $\hat{\eta}_{V,b}$ of a thermal pure quantum state $|\psi_\beta\rangle$, with mean-squared error σ_j^2 [Eq. (8) or (9)] for observable O_j , are sufficient to estimate all M Gibbs state expectation values, $\text{Tr} \rho_\beta O_j$, with a success probability of at least $1 - \delta$, i.e.,

$$\Pr \left[\max_j |\mu_j(N, K) - \text{Tr} \rho_\beta O_j| \leq \epsilon \right] \geq 1 - \delta. \quad (11)$$

Here $\mu_j(N, K)$ is the predicted expectation value for observable O_j obtained from a median-of-means estimation on K subsets of N classical shadows. A detailed proof of this Theorem and a review of Theorem 1 in Ref. [23] is given in the SM. We conclude that for M Gibbs state expectation values we require $\mathcal{O}(\log M)$ preparations of TPQ states $|\psi_\beta\rangle$ and randomized measurements. The exact performance of the algorithm depends on which type of measurement one uses (Pauli or Clifford) and the considered observables. For k -local Pauli observables, with $k \ll n$, the variance of Pauli measurements [Eq. (9)], is lower and hence a better choice. On the other hand, for tasks like fidelity estimation the Clifford measurements perform better [23].

Implementation – In order to implement the pure thermal shadow algorithm on a quantum device we need several different elements. Firstly, we need a method to sample uniformly from the n -qubit Clifford group to generate the random Clifford circuits U . An efficient, polynomial-time, algorithm exists for this [40], which has been implemented in the quantum computing library `qiskit`. We can use this for both the generation of the random pure states at the beginning of the algorithm as well as the randomized measurements at the end. Secondly, we need a method for approximating the non-unitary operator $e^{-\beta H/2}$ in Eq. (2). To this end, we use quantum signal processing [31] (QSP), a framework for performing matrix arithmetics on quantum computers.

We assume the Hamiltonian is given in the form $H = \sum_k a_k P_k$ where $a_k \in \mathbb{R}$ and P_k are n -qubit Pauli operators. QSP requires a block-encoding of the Hamiltonian into a larger unitary matrix [41]. In turn, this requires a preprocessing step that rescales the spectrum of H to the interval $[0, 1]$. We achieve this with a min-max rescaling $\tilde{H} = (H - \lambda_{\min} \mathbb{1}) / (\lambda_{\max} - \lambda_{\min})$ where λ_{\min} (λ_{\max}) is the smallest (largest) eigenvalue. In practice, the extremal eigenvalues are unknown and one resorts to a lower bound for λ_{\min} and to an upper bound for λ_{\max} . We also define the imaginary time $\tau = \beta(\lambda_{\max} - \lambda_{\min})/2$ so that

$$e^{-\tau \tilde{H}} = e^{-\beta \lambda_{\min}/2} e^{-\beta H/2}. \quad (12)$$

Thus, we can evolve \tilde{H} for time τ and obtain the desired non-unitary operator up to a constant factor. This factor is irrelevant as it cancels out in Eq. (2).

We then use QSP to implement a polynomial approximation to the exponential function, and apply it

to the eigenvalues of \tilde{H} [42, 43]. The method in Ref. [42], Corollary 64, approximates the exponential function to accuracy ϵ with a polynomial of degree $\mathcal{O}(\sqrt{\beta}(\lambda_{\max} - \lambda_{\min})\log(1/\epsilon))$. The degree is proportional to the number of uses of the block-encoding circuit and thus determines the overall depth of the circuit. In our implementation, we instead numerically find a polynomial approximation to $e^{-\tau|x|}$ using the `pyqsp` library [32] and then construct a suitable QSP circuit.

At the bottom of Fig. 1, we show the circuit diagram for the pure thermal shadow algorithm. The success probability $\|e^{-\tau\tilde{H}}U|0\rangle\|^2$ depends on the random Clifford circuit U . Averaging over the Clifford group and using Eq. (12) we find that the probability of success is $\mathcal{O}(e^{\beta\lambda_{\min}}\text{Tre}^{-\beta H}/2^n)$. It can be verified that the success probability decreases as β increases. This is expected from the intuition that low-temperature sampling is computationally harder. By including $\mathcal{O}(e^{-\beta\lambda_{\min}/2}\sqrt{2^n}/\text{Tre}^{-\beta H})$ iterations of amplitude amplification, the protocol is enhanced and succeeds with probability $\mathcal{O}(1)$. Amplitude amplification can be implemented via yet another layer of QSP [32]. Note that while this protocol works for any Hamiltonian and temperature, the total circuit depth is expected to be polynomial in n only for certain choices of H and β .

Numerical demonstration – We simulate the circuit for the one-dimensional XXZ-Heisenberg Hamiltonian [33, 34] given by

$$H = \sum_{i=1}^{n-1} J (\sigma_i^x \sigma_{i+1}^x + \sigma_i^y \sigma_{i+1}^y) + \Delta \sigma_i^z \sigma_{i+1}^z. \quad (13)$$

Here J is the nearest-neighbor x, y -coupling constant and Δ is the nearest-neighbor z -coupling strength. This is a paradigmatic model for the study of (quantum) magnetism and it maps to the Hubbard model for spinless interacting Fermions after a Jordan-Wigner transformation. We set the system size to $n = 10$ and the coupling parameters to $J = 0.5$ and $\Delta = 0.75$, which means the ground state is in the anti-ferromagnetic phase [34].

First, in Fig. 2(a) we show the maximum error of the estimated expectation values of all one- and two-qubit Pauli observables (435 in total) using the TPQ states in Eq. (3) generated with QSP. Note that here we use the full TPQ statevectors to estimate the expectation values and have not constructed thermal shadows yet. We observe that the error goes down if we increase the degree of the polynomial approximation used in QSP. This shows that we can use QSP to tune the accuracy. In addition, we see that, as expected, the method performs better for higher temperatures, i.e., smaller β .

In Fig. 2(b) we show the same error computed for the full algorithm, in which we use the mean expectation values of the thermal shadows to estimate the true Gibbs state expectation values. As we are computing Pauli observables we use random Pauli measurements

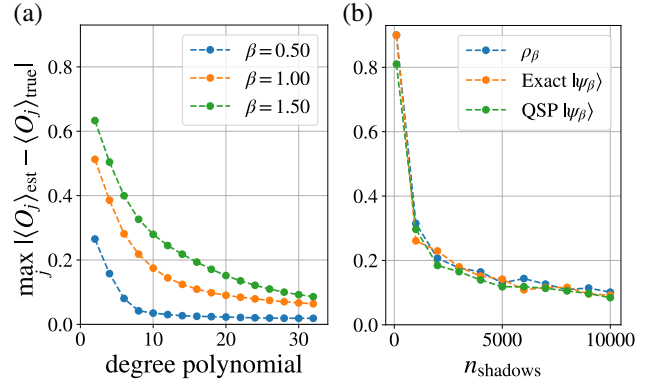


FIG. 2. Maximum error between the exact Gibbs state expectation values, $\langle O_j \rangle_{\text{true}} = \text{Tr} O_j \rho_\beta$, and the estimated expectation values $\langle O_j \rangle_{\text{est}}$ for all possible one- and two-qubit Pauli operators O_j . In (a) we estimate the expectation values directly on thermal pure quantum states, $|\psi_\beta\rangle$, generated with QSP for different inverse temperatures β as function of the degree of the polynomial approximation. In (b) we compare the errors between shadows constructed directly from the true Gibbs state, ρ_β , and shadows constructed from the exact TPQ states and the TPQ states generated with QSP.

for this. We compare the performance of shadows constructed from the exact Gibbs state ρ_β with $\beta = 1$, the exact TPQ state, and the TPQ state obtained from a QSP of degree 32. As we increase the number of shadows used to estimate the expectation values, we observe that the maximum error becomes similar, $\mathcal{O}(10^{-1})$, for all three methods. This confirms our theoretical finding that shadows constructed from $|\psi_\beta\rangle$ perform as well as shadows constructed from ρ_β .

Summary and outlook – In this Letter we show that one can predict M linear properties of a Gibbs state at finite temperature with only $\mathcal{O}(\log M)$ preparations of a thermal pure state. In practice this means one only needs to prepare a n -qubit random pure state on a quantum device, imaginary time evolve it with the system Hamiltonian and finally perform randomized measurements. Compared to algorithms that prepare a purification of the Gibbs state, our approach reduces the required qubits by a half. We propose an implementation of our algorithm where the imaginary time evolution is performed by quantum signal processing. By simulating a XXZ-Heisenberg model we demonstrate the performance of the algorithm and circuit.

For future studies a few interesting avenues can be investigated. One can look at constructing shadows of other types of thermal pure states, such as states that satisfy the eigenstate thermalization hypothesis [1, 44] and minimally entangled typical thermal states [9]. Another option is to look at the generalization to other thermodynamic ensembles. In addition, one can investigate further improvements of the algorithm by derandomization [45] of the measurements and also the prediction

of nonlinear functions of ρ_β . Lastly, we foresee the use of our algorithm as a subroutine in quantum algorithms that require the evaluation of Gibbs state expectation values, such as quantum semi-definite programming and quantum Boltzmann machines.

Acknowledgments: We thank David Amaro, Samuel Duffield, Mattia Fiorentini, Masaru Hongo, Bert Kappen, Michael Lubasch, Stefano Mangini, and Kirill Plekhanov for helpful discussions. We thank Nathan Fitzpatrick, Matthias Rosenkranz, and Chris Self for providing feedback on a earlier version of this manuscript.

* luuk.coopmans@cambridgequantum.com

- [1] C. Gogolin and J. Eisert, Equilibration, thermalisation, and the emergence of statistical mechanics in closed quantum systems, *Reports on Progress in Physics* **79**, 056001 (2016).
- [2] Á. M. Alhambra, Quantum many-body systems in thermal equilibrium (2022), [arXiv:2204.08349 \[quant-ph\]](https://arxiv.org/abs/2204.08349).
- [3] E. Y. Loh, J. E. Gubernatis, R. T. Scalettar, S. R. White, D. J. Scalapino, and R. L. Sugar, Sign problem in the numerical simulation of many-electron systems, *Phys. Rev. B* **41**, 9301 (1990).
- [4] M.-H. Yung and A. Aspuru-Guzik, A quantum–quantum metropolis algorithm, *Proceedings of the National Academy of Sciences* **109**, 754 (2012).
- [5] A. N. Chowdhury and R. D. Somma, Quantum algorithms for gibbs sampling and hitting-time estimation (2016), [arXiv:1603.02940 \[quant-ph\]](https://arxiv.org/abs/1603.02940).
- [6] S. Endo, J. Sun, Y. Li, S. C. Benjamin, and X. Yuan, Variational quantum simulation of general processes, *Phys. Rev. Lett.* **125**, 010501 (2020).
- [7] J.-G. Liu, L. Mao, P. Zhang, and L. Wang, Solving quantum statistical mechanics with variational autoregressive networks and quantum circuits, *Machine Learning: Science and Technology* **2**, 025011 (2021).
- [8] J. R. McClean, S. Boixo, V. N. Smelyanskiy, R. Babush, and H. Neven, Barren plateaus in quantum neural network training landscapes, *Nature Communications* **9**, 4812 (2018).
- [9] S. R. White, Minimally entangled typical quantum states at finite temperature, *Phys. Rev. Lett.* **102**, 190601 (2009).
- [10] M. Motta, C. Sun, A. T. K. Tan, M. J. O’Rourke, E. Ye, A. J. Minnich, F. G. S. L. Brandão, and G. K.-L. Chan, Determining eigenstates and thermal states on a quantum computer using quantum imaginary time evolution, *Nature Physics* **16**, 205 (2020).
- [11] P. Bocchieri and A. Loinger, Ergodic foundation of quantum statistical mechanics, *Phys. Rev.* **114**, 948 (1959).
- [12] A. Hams and H. De Raedt, Fast algorithm for finding the eigenvalue distribution of very large matrices, *Phys. Rev. E* **62**, 4365 (2000).
- [13] S. Popescu, A. J. Short, and A. Winter, Entanglement and the foundations of statistical mechanics, *Nature Physics* **2**, 754 (2006).
- [14] S. Sugiura and A. Shimizu, Thermal pure quantum states at finite temperature, *Phys. Rev. Lett.* **108**, 240401 (2012).
- [15] S. Sugiura and A. Shimizu, Canonical thermal pure quantum state, *Phys. Rev. Lett.* **111**, 010401 (2013).
- [16] M. Hyuga, S. Sugiura, K. Sakai, and A. Shimizu, Thermal pure quantum states of many-particle systems, *Phys. Rev. B* **90**, 121110 (2014).
- [17] H. Endo, C. Hotta, and A. Shimizu, From linear to nonlinear responses of thermal pure quantum states, *Phys. Rev. Lett.* **121**, 220601 (2018).
- [18] F. Jin, D. Willsch, M. Willsch, H. Lagemann, K. Michielsen, and H. D. Raedt, Random state technology, *Journal of the Physical Society of Japan* **90**, 012001 (2021).
- [19] A. Iwaki, A. Shimizu, and C. Hotta, Thermal pure quantum matrix product states recovering a volume law entanglement, *Physical Review Research* **3** (2021).
- [20] S. Tsutsui, M. Hongo, S. Sato, and T. Sagawa, Quantum hydrodynamics from local thermal pure states (2021), [arXiv:2106.12777 \[cond-mat.stat-mech\]](https://arxiv.org/abs/2106.12777).
- [21] S. Aaronson, Shadow tomography of quantum states (2017), [arXiv:1711.01053 \[quant-ph\]](https://arxiv.org/abs/1711.01053).
- [22] M. Pains and A. Kalev, An approximate description of quantum states (2019), [arXiv:1910.10543 \[quant-ph\]](https://arxiv.org/abs/1910.10543).
- [23] H.-Y. Huang, R. Kueng, and J. Preskill, Predicting many properties of a quantum system from very few measurements, *Nature Physics* **16**, 1050 (2020).
- [24] R. Levy, D. Luo, and B. K. Clark, Classical shadows for quantum process tomography on near-term quantum computers (2021), [arXiv:2110.02965 \[quant-ph\]](https://arxiv.org/abs/2110.02965).
- [25] J. Kunjummen, M. C. Tran, D. Carney, and J. M. Taylor, Shadow process tomography of quantum channels (2021), [arXiv:2110.03629 \[quant-ph\]](https://arxiv.org/abs/2110.03629).
- [26] M. McGinley, S. Leontica, S. J. Garratt, J. Jovanovic, and S. H. Simon, Quantifying information scrambling via classical shadow tomography on programmable quantum simulators (2022), [arXiv:2202.05132 \[quant-ph\]](https://arxiv.org/abs/2202.05132).
- [27] A. Elben, S. T. Flammia, H.-Y. Huang, R. Kueng, J. Preskill, B. Vermersch, and P. Zoller, The randomized measurement toolbox (2022), [arXiv:2203.11374 \[quant-ph\]](https://arxiv.org/abs/2203.11374).
- [28] A. Ambainis and J. Emerson, Quantum t-designs: t-wise independence in the quantum world (2007), [arXiv:quant-ph/0701126 \[quant-ph\]](https://arxiv.org/abs/quant-ph/0701126).
- [29] G. H. Low, T. J. Yoder, and I. L. Chuang, Methodology of resonant equiangular composite quantum gates, *Physical Review X* **6** (2016).
- [30] G. H. Low and I. L. Chuang, Optimal hamiltonian simulation by quantum signal processing, *Physical Review Letters* **118** (2017).
- [31] G. H. Low and I. L. Chuang, Hamiltonian simulation by qubitization, *Quantum* **3**, 163 (2019).
- [32] J. M. Martyn, Z. M. Rossi, A. K. Tan, and I. L. Chuang, Grand unification of quantum algorithms, *PRX Quantum* **2**, 040203 (2021).
- [33] W. Heisenberg, Zur theorie des ferromagnetismus, *Zeitschrift für Physik* **49**, 619 (1928).
- [34] F. Franchini, *An Introduction to Integrable Techniques for One-Dimensional Quantum Systems* (Springer International Publishing, 2017).
- [35] Z. Webb, The clifford group forms a unitary 3-design (2015), [arXiv:1510.02769 \[quant-ph\]](https://arxiv.org/abs/1510.02769).
- [36] S. Aaronson and D. Gottesman, Improved simulation of stabilizer circuits, *Physical Review A* **70** (2004).
- [37] We assume that the system size is large enough for the contributions from boundaries to be negligible.

- [38] Note that this includes most observables that one typically considers in a physical setting, e.g. any k -local Pauli operator with $k \ll n$.
- [39] For a general k -local operator O , the Pauli mean-squared error is bounded as $\sigma^2 \leq 4^k \|O_0\|^2 - (\mathbb{E}_U[\langle \psi_\beta | O_0 | \psi_\beta \rangle])^2 + \mathcal{O}(e^{-n})$.
- [40] S. Bravyi and D. Maslov, Hadamard-free circuits expose the structure of the clifford group, *IEEE Transactions on Information Theory* **67**, 4546 (2021).
- [41] The block-encoding circuit is problem specific and won't be discussed here. There exist generic block-encoding schemes for Hamiltonians.
- [42] A. Gilyén, Y. Su, G. H. Low, and N. Wiebe, Quantum singular value transformation and beyond: exponential improvements for quantum matrix arithmetics, in *Proceedings of the 51st Annual ACM SIGACT Symposium on Theory of Computing* (ACM, 2019).
- [43] J. van Apeldoorn, A. Gilyén, S. Gribling, and R. de Wolf, Quantum SDP-solvers: Better upper and lower bounds, *Quantum* **4**, 230 (2020).
- [44] M. Srednicki, Chaos and quantum thermalization, *Physical Review E* **50**, 888 (1994).
- [45] H.-Y. Huang, R. Kueng, and J. Preskill, Efficient estimation of pauli observables by derandomization, *Physical Review Letters* **127** (2021).
- [46] D. Gottesman, Stabilizer codes and quantum error correction (1997), [arXiv:quant-ph/9705052 \[quant-ph\]](#).
- [47] D. Gottesman, The heisenberg representation of quantum computers (1998), [arXiv:quant-ph/9807006 \[quant-ph\]](#).
- [48] M. Lerasle, Lecture notes: Selected topics on robust statistical learning theory (2019), [arXiv:1908.10761 \[stat.ML\]](#).
- [49] Y.-C. Chen, *A short note on the median-of-means estimator* (2020).

Supplemental Material

Predicting Gibbs State Expectation Values with Pure Thermal Shadows

REVIEW OF CLASSICAL SHADOWS

Here we review classical shadow tomography, which was originally introduced by Aaronson [21] and later on made into a practical protocol by Pains and Kalev [22] and Huang *et al.* [23]. This method uses randomized measurements to construct efficient classical representations (shadows) of an arbitrary quantum state ρ . The power of this randomized approach is that it can be used to predict many properties (such as observables) of ρ with very few measurements. We start by outlining all the steps in this randomized measurement method (by following Ref. [23]) and defining what the classical shadows are. Afterwards, we prove how many shadows are required to compute M expectation values, $\text{Tr} \rho O_j$, for a set of arbitrary observables $\{O_j\}_{j=1}^M$.

Randomized measurements and classical shadows

Definition 1. (*Randomized Measurements*): Given an arbitrary n -qubit quantum state ρ and a random unitary operator U , which is drawn uniformly from some ensemble \mathcal{U} , we define a random measurement process as follows:

$$\rho \mapsto U \rho U^\dagger \mapsto |b\rangle\langle b|, \quad (14)$$

where in the second step we have measured in the computational basis, i.e., b is a bit string. The probability of obtaining bit string b is given by Born's rule:

$$\text{Tr}[U \rho U^\dagger |b\rangle\langle b|] = \langle b|U \rho U^\dagger |b\rangle. \quad (15)$$

The interpretation of this measurement process is straightforward: we rotate the quantum state to some random basis and then perform a computational basis measurement. Taking these two steps together, we have thus performed a measurement in a random basis.

This random measurement process can then be used to construct efficient classical representations of ρ by performing some (classical) post-processing steps. First, one applies the inverse of U to the outcome $|b\rangle\langle b|$. This can be done classically efficiently if U was drawn, for example, from the n -qubit Clifford group $\text{Cl}(2^n)$, or a tensor product of random single-qubit Cliffords, $U = U_1 \otimes \dots \otimes U_n$, where $U_i \in \text{Cl}(2)$. We then repeat this measurement process many times, each time for a different unitary U , and look at the expectation value, $\mathbb{E}[U^\dagger |b\rangle\langle b| U]$. We can see that this complete process defines a quantum channel \mathcal{M} on the original state ρ . Specifically, we get

$$\mathbb{E}[U^\dagger |b\rangle\langle b| U] = \mathbb{E}_{U \in \mathcal{U}} \sum_{b \in \{0,1\}^n} \langle b|U \rho U^\dagger |b\rangle U^\dagger |b\rangle\langle b| U \equiv \mathcal{M}(\rho). \quad (16)$$

As \mathcal{M} is a linear map, we can obtain information about ρ from the measurement results by inverting the channel \mathcal{M}^{-1} . We remark that the channel is invertible provided that the map is one-to-one. This means that there exists a unitary $U \in \mathcal{U}$, and a corresponding b , for which $\langle b|U \rho U^\dagger |b\rangle \neq \langle b|U \sigma U^\dagger |b\rangle$ for $\rho \neq \sigma$. Applying \mathcal{M}^{-1} to both sides of Eq. (16) gives

$$\mathbb{E}[\mathcal{M}^{-1}(U^\dagger |b\rangle\langle b| U)] = \rho. \quad (17)$$

Note that here we have used the fact that \mathcal{M}^{-1} is a linear map and hence can be absorbed into the expectation value. From this we can define the classical shadows.

Definition 2. (*Classical Shadow*): Given a n -qubit quantum state ρ and a bit string $|b\rangle$ obtained from a randomized measurement of ρ with random unitary $U \in \mathcal{U}$. A classical shadow of the state ρ is defined to be the unit-trace operator

$$\hat{\rho}_{U,b} = \mathcal{M}^{-1}(U^\dagger |b\rangle\langle b| U), \quad (18)$$

provided that there exists a unitary $U \in \mathcal{U}$ and a corresponding b for which $\langle b|U \rho U^\dagger |b\rangle \neq \langle b|U \sigma U^\dagger |b\rangle$ for $\rho \neq \sigma$.

By definition, these classical shadows reproduce the quantum state ρ if we average over the unitaries U and measurement outcomes b , i.e., $\mathbb{E}[\hat{\rho}_{U,b}] = \rho$. However, in order to efficiently store and compute these shadows classically, we need to derive the explicit form of the channel \mathcal{M} . We will do this in the next subsection for random Clifford unitaries $U \in \text{Cl}(2^n)$.

The inverse quantum channel, \mathcal{M}^{-1} , for randomized Clifford measurements

To construct \mathcal{M}^{-1} we evaluate the effect of the channel \mathcal{M} on an arbitrary state ρ ,

$$\mathcal{M}(\rho) = \mathbb{E}_{U \in \mathcal{U}} \sum_{b \in \{0,1\}^n} \langle b|U\rho U^\dagger|b\rangle U^\dagger|b\rangle \langle b|U = \sum_{b \in \{0,1\}^n} \mathbb{E}_{U \in \mathcal{U}} \langle b|U\rho U^\dagger|b\rangle U^\dagger|b\rangle \langle b|U. \quad (19)$$

Evaluating this expression for any arbitrary ensemble \mathcal{U} is very hard, if possible at all. However, we recognize that the argument of the average over the ensemble \mathcal{U} is a polynomial of order 2 in (U, U^\dagger) . This means that if the unitary U is at least a unitary 2-design [28] we can replace the inner average by an integral with respect to the Haar measure $d\mu_{\text{Haar}}(U)$,

$$\sum_{b \in \{0,1\}^n} \mathbb{E}_{U \in \mathcal{U}_{k \geq 2}} \langle b|U\rho U^\dagger|b\rangle U^\dagger|b\rangle \langle b|U = \sum_{b \in \{0,1\}^n} \int_{U \in \mathcal{U}} d\mu_{\text{Haar}}(U) \langle b|U\rho U^\dagger|b\rangle U^\dagger|b\rangle \langle b|U, \quad (20)$$

where $\mathbb{E}_{U \in \mathcal{U}_{k \geq 2}}$ is the average over a unitary k -design. An example of a unitary 3-design, and thus also a 2-design, are the random Clifford unitaries, $U \in \text{Cl}(2^n)$ [35], that can be classically simulated and sampled efficiently by the Gottesmann-Knill theorem [46, 47]. For this reason, from now on we use random n -qubit Clifford measurements. However, in reality we can use any randomized measurements with a unitary $k \geq 2$ -design.

The advantage of writing the average as a Haar integral is that expressions exist to evaluate some integrals analytically. In particular, in the following we repeatedly make use of the following three Haar-integral identities [23]:

$$\int_{U \in \mathcal{U}} d\mu_{\text{Haar}}(U) \langle b|U O_1 U^\dagger|b\rangle = \frac{\text{Tr} O_1}{2^n}. \quad (21)$$

$$\int_{U \in \mathcal{U}} d\mu_{\text{Haar}}(U) U^\dagger|b\rangle \langle b|U \langle b|U O_1 U^\dagger|b\rangle = \frac{O_1 + \mathbb{1} \text{Tr} O_1}{2^n(2^n + 1)}. \quad (22)$$

$$\int_{U \in \mathcal{U}} d\mu_{\text{Haar}}(U) U^\dagger|b\rangle \langle b|U \langle b|U O_2 U^\dagger|b\rangle \langle b|U O_3 U^\dagger|b\rangle = \frac{\mathbb{1} \text{Tr}[O_2 O_3] + O_2 O_3 + O_3 O_2}{2^n(2^n + 1)(2^n + 2)}. \quad (23)$$

Here O_1 is an arbitrary Hermitian operator, and, O_2 and O_3 are trace-less operators.

Using the 2nd moment Haar integral, Eq. (22), we find

$$\sum_{b \in \{0,1\}^n} \int_{U \in \mathcal{U}} d\mu_{\text{Haar}}(U) \langle b|U\rho U^\dagger|b\rangle U^\dagger|b\rangle \langle b|U = \frac{\rho + \mathbb{1} \text{Tr} \rho}{(2^n + 1)}. \quad (24)$$

This leads to the following inverse quantum channel for $U \in \mathcal{U}_{k \geq 2}$,

$$\mathcal{M}(\rho) = \frac{\rho + \mathbb{1} \text{Tr} \rho}{(2^n + 1)} \implies \mathcal{M}^{-1}(X) = (2^n + 1)X - \mathbb{1} \text{Tr} X, \quad (25)$$

where we used the fact that the channel is unital, $\mathcal{M}(\mathbb{1}) = \mathbb{1}$, and X is a hermitian operator of dimension $2^n \times 2^n$. As such, the classical shadows (18) for random n -qubit Clifford measurements of the state ρ are given by

$$\hat{\rho}_{U,b} = (2^n + 1)U^\dagger|b\rangle \langle b|U - \mathbb{1}. \quad (26)$$

Computing expectation values with Classical Shadows

Having defined the classical shadows and shown how to construct them from outcomes of randomized measurements, we can now look into the problem of computing expectation values. Suppose we are interested in expectation values of the form $\text{Tr} \rho O_j$, for the set of Hermitian operators $\{O_j\}_{j=1}^M$. In this subsection, we show that we can compute these expectation values by taking the classical shadows, $\hat{\rho}_{U,b}$, as estimators for the density matrix. To keep this review concise, we will only focus on the randomized Clifford measurements, for which the shadows are given in Eq. (26).

In order to show that we can use $\hat{\rho}_{U,b}$ as an estimator for the expectation values of ρ we need to compute the average, $\mathbb{E}[\text{Tr} \hat{\rho}_{U,b} O_j]$, and the variance, $\text{Var}[\text{Tr} \hat{\rho}_{U,b} O_j]$, with respect to the randomized measurement process. As

the estimators $\hat{\rho}_{U,b}$ are obtained from randomized Clifford measurements, we can compute these averages by again exploiting the fact that $U \in \mathcal{Cl}(2^n)$ is a unitary 3-design. Firstly, by using the linearity of the trace and Eq. (17), we find

$$\mathbb{E}[\text{Tr}\hat{\rho}_{U,b}O_j] = \text{Tr}\mathbb{E}[\hat{\rho}_{U,b}]O_j = \text{Tr}\rho O_j \quad (27)$$

for the average of the shadow expectation value of observable O_j . For the computation of the variance, we note that it only depends on the trace-less part, $O_j^0 = O_j - \frac{1}{2^n}\text{Tr}O_j$, of O_j . This can be seen from

$$\text{Var}[\text{Tr}\hat{\rho}_{U,b}O_j] = \mathbb{E}[(\text{Tr}\hat{\rho}_{U,b}O_j - \mathbb{E}[\text{Tr}\hat{\rho}_{U,b}O_j])^2] = \mathbb{E}[(\text{Tr}\hat{\rho}_{U,b}O_j^0)^2] - (\text{Tr}\rho O_j^0)^2. \quad (28)$$

This important observation has simplified the variance calculation enormously, as we now only need to compute one Haar integral. Focusing on the first term in the variance, we get

$$\mathbb{E}[(\text{Tr}\hat{\rho}_{U,b}O_j^0)^2] = \mathbb{E}[(\text{Tr}\mathcal{M}^{-1}(U^\dagger|b\rangle\langle b|U)O_j^0)^2] \quad (29)$$

$$= (2^n + 1)^2 \sum_{b \in \{0,1\}^n} \int_{U \in \mathcal{U}} d\mu_{\text{Haar}}(U) \text{Tr}\rho U^\dagger|b\rangle\langle b|U \langle b|U O_j^0 U^\dagger|b\rangle^2 \quad (30)$$

$$= \frac{2^n + 1}{2^n + 2} (\text{Tr}(O_j^0)^2 + 2\text{Tr}\rho(O_j^0)^2). \quad (31)$$

Here we have used the identity for the 3rd moment Haar integral (23) for trace-less operators after swapping the trace and integral in Eq. (30). Subsequently, we performed the sum over all bit strings to obtain the result in Eq. (31). The variance is thus equal to

$$\text{Var}[\text{Tr}\hat{\rho}_{U,b}O_j] = \frac{2^n + 1}{2^n + 2} (\text{Tr}(O_j^0)^2 + 2\text{Tr}\rho(O_j^0)^2) - (\text{Tr}\rho O_j^0)^2. \quad (32)$$

Predicting M observables with $\mathcal{O}(\log M)$ classical shadows

For the final part of our review of the classical shadow tomography algorithm, we show that we only need $\mathcal{O}(\log M)$ independent classical shadows, $\hat{\rho}_{U,b}$, to predict M expectation values $\{\text{Tr}\rho O_j\}_{j=1}^M$. To simplify the notation we replace the U and b subscripts with an index; that is, now $\hat{\rho}_i$ denotes the i -th shadow. We follow the approach laid out in Ref. [23] closely and perform a median-of-means estimation. The median-of-means estimator of $\text{Tr}\rho O_j$ is defined as

$$\mu_j(N, K) = \text{median}[\mu_j^1(N), \mu_j^2(N), \dots, \mu_j^K(N)], \quad (33)$$

with

$$\mu_j^k(N) = \frac{1}{N} \sum_{i=N(k-1)+1}^{Nk} \text{Tr}\hat{\rho}_i O_j. \quad (34)$$

This means that we construct in total $n_{\text{shadows}} = NK$ independent shadows $\hat{\rho}_i$, divide them into K subsets of size N , compute the mean of each subset, and finally take the median of the subset means.

Although this procedure is slightly more complicated than computing the mean directly on all the shadows, there are scenarios in which the median-of-means estimator is a more robust estimator than the standard mean estimator (see e.g. [48]). Moreover, results are known for how many samples (independent estimators) are required to predict a function up to a certain accuracy. Specifically, for a random variable X with finite sample variance σ^2 , the median-of-means estimator, $\tilde{\mu}(N, K)$, has the following failure probability [48, 49],

$$\Pr[|\tilde{\mu}(N, K) - \mathbb{E}[X]| \geq \epsilon] \leq e^{-2K\left(\frac{1}{2} - \frac{\sigma^2}{N\epsilon^2}\right)^2}, \quad (35)$$

where the number of shadows in each subset needs to satisfy $N > 2\sigma^2/\epsilon^2$ for this inequality to hold. Then, by setting $K = (9/2)\log(M/\delta)$ and $N = 6\sigma^2/\epsilon^2$, we find

$$\Pr[|\tilde{\mu}(N, K) - \mathbb{E}[X]| \geq \epsilon] \leq \frac{\delta}{M}. \quad (36)$$

The values of the constants N and K are found by minimizing the number of shadows for a fixed upper bound δ/M and with $N > 2\sigma^2/\epsilon^2$. This way we obtain a number of shadows $n_{\text{shadows}} = NK$ smaller than the (reserved) one found in Ref. [45].

Now by applying a median-of-means estimation to the problem of computing M observables O_j we find

$$\Pr[|\mu_j(N, K) - \text{Tr}\rho O_j| \geq \epsilon] \leq \frac{\delta}{M}. \quad (37)$$

As this is the failure probability for each individual observable O_j , the failure probability of all of them together (i.e., that at least one observable fails) follows from Boole's inequality,

$$\Pr\left[\max_{j \in \{1, \dots, M\}} |\mu_j(N, K) - \text{Tr}\rho O_j| \geq \epsilon\right] \leq \delta. \quad (38)$$

From this we arrive at the following theorem [23].

Theorem 2. (*Number of shadows for M observables*): Given a random measurement process with unitary ensemble \mathcal{U} , M Hermitian operators O_j , and accuracy parameters $\epsilon, \delta \in [0, 1]$, in total

$$n_{\text{shadows}} = NK = \frac{27 \log(M/\delta)}{\epsilon^2} \max_j [\sigma_j^2] \quad (39)$$

classical shadows $\hat{\rho}$, with σ_j^2 the shadow variance (Eq. (32) for Cliffords) for observable O_j , are sufficient to estimate all M expectation values, $\text{Tr}\rho O_j$, with a success probability of

$$\Pr\left[\max_{j \in \{1, \dots, M\}} |\mu_j(N, K) - \text{Tr}\rho O_j| \leq \epsilon\right] \geq 1 - \delta. \quad (40)$$

This means that in total we need $\mathcal{O}(\log M)$ randomized measurements. Importantly, the mean-squared error for observable O_j , σ_j^2 , depends on the operator that one tries to measure, and which specific unitary ensemble is used. As a final remark, note that the constants in Eq. (39) result from bounding the failure probability. This means that it is a worst case scenario (upper bound), and in practice one could likely get away with fewer shadows.

PROOF OF EXPONENTIALLY VANISHING FAILURE PROBABILITY OF THERMAL PURE QUANTUM STATES

In this section we show that the random state

$$|\psi_\beta\rangle = \frac{e^{-\beta H/2} U |0\rangle}{\sqrt{\langle 0|U^\dagger e^{-\beta H} U|0\rangle}}, \quad (41)$$

where the unitary $U \in \mathcal{U}_{k \geq 2}$ is at least a quantum 2-design, satisfies Eq. (1) in the main text and therefore is a thermal pure quantum (TPQ) state. We start by deriving the expectation value and variance of an observable O in the state $|\psi_\beta\rangle$, for which the results are given in Eqs. (3) and (4) in the main text. Afterward, we apply Markov's inequality to prove the exponentially vanishing failure probability.

Deriving the variance and expectation value of the thermal pure quantum state

Firstly, we note that the variance of the normalization constant, $\langle 0|U^\dagger e^{-\beta H} U|0\rangle$, of the TPQ state, $|\psi_\beta\rangle$, is exponentially suppressed. This can be derived by evaluating the variance explicitly and invoking the Haar integral identities in Eqs. (21) and (22),

$$\text{Var}[\langle 0|U^\dagger e^{-\beta H} U|0\rangle] = \mathbb{E}_U[\langle 0|U^\dagger e^{-\beta H} U|0\rangle^2] - (\mathbb{E}_U[\langle 0|U^\dagger e^{-\beta H} U|0\rangle])^2 = \frac{2^n \text{Tr} e^{-2\beta H} - (\text{Tr} e^{-\beta H})^2}{2^{2n}(2^n + 1)}. \quad (42)$$

Since $1 \leq \text{Tr} e^{-2\beta H} \leq 2^n$ for all β , this variance will always be exponentially small in the system size, n .

In the following we use the shorthand notation, $f \equiv \langle 0|U^\dagger e^{-\beta H/2} O e^{-\beta H/2} U|0\rangle$ and $g \equiv \langle 0|U^\dagger e^{-\beta H} U|0\rangle$. As $\text{Var}[g]$ is small, we expand the expectation value of O with a multivariate Taylor expansion up to first order in $\text{Var}[g]$,

$$\mathbb{E}[\langle \psi_\beta | O | \psi_\beta \rangle] = \mathbb{E}\left[\frac{f}{g}\right] \approx \frac{\mathbb{E}[f]}{\mathbb{E}[g]} - \frac{\text{Cov}[f, g]}{\mathbb{E}[g]^2} + \frac{\mathbb{E}[f]}{\mathbb{E}[g]^3} \text{Var}[g], \quad (43)$$

where $\text{Cov}[f, g]$ stands for the covariance between f and g defined by $\text{Cov}[f, g] \equiv \mathbb{E}[fg] - \mathbb{E}[f]\mathbb{E}[g]$. Now by evaluating each of the terms in this Taylor expansion with the Haar integral identities in Eqs. (21) and (22), we arrive at Eq. (3) in the main text,

$$\mathbb{E}[\langle \psi_\beta | O | \psi_\beta \rangle] \approx \text{Tr} \rho_\beta O + \text{Tr} \rho_\beta^2 (\text{Tr} \rho_\beta O - \text{Tr} \rho_{2\beta} O). \quad (44)$$

For the variance of the expectation value we exploit a similar multivariate Taylor expansion,

$$\text{Var}\left[\frac{f}{g}\right] \approx \frac{\text{Var}[f]}{\mathbb{E}[g]^2} - \frac{2\mathbb{E}[f]}{\mathbb{E}[g]^3} \text{Cov}[f, g] + \frac{\mathbb{E}[f]^2}{\mathbb{E}[g]^4} \text{Var}[g], \quad (45)$$

and obtain Eq. (4) in the main text after the evaluation of the Haar integrals,

$$\text{Var}[\langle \psi_\beta | O | \psi_\beta \rangle] \approx \text{Tr} \rho_\beta^2 \left(\frac{(\text{Tr}(O e^{-\beta H}))^2}{\text{Tr} e^{-2\beta H}} - 2\text{Tr} \rho_\beta O \text{Tr} \rho_{2\beta} O + (\text{Tr} \rho_\beta O)^2 \right). \quad (46)$$

Application of Markov's inequality

In order to show that $|\psi_\beta\rangle$ satisfies Eq. (1) in the main text, we start from the following Markov inequality,

$$\Pr[|\langle \psi_\beta | O | \psi_\beta \rangle - \text{Tr} \rho_\beta O| \geq \epsilon] \leq \frac{\mathbb{E}_U[|\langle \psi_\beta | O | \psi_\beta \rangle - \text{Tr} \rho_\beta O|^2]}{\epsilon^2} \quad (47)$$

Here \mathbb{E}_U denotes the ensemble average with respect to the n -qubit Clifford group $U \in \text{Cl}(2^n)$. This average can be computed by using the unitary 2-design property of U and writing it in terms of Haar integrals. After evaluating the integrals, this results in

$$\mathbb{E}_U[|\langle \psi_\beta | O | \psi_\beta \rangle - \text{Tr} \rho_\beta O|^2] = \text{Tr} \rho_\beta^2 \left(\frac{(\text{Tr}(O e^{-\beta H}))^2}{\text{Tr} e^{-2\beta H}} - 2\text{Tr} \rho_\beta O \text{Tr} \rho_{2\beta} O - (\text{Tr} \rho_\beta O)^2 \right). \quad (48)$$

The terms that multiply the purity, $\text{Tr} \rho_\beta^2$, in this expression, have the form of expectation values, which can be upper bounded by the spectral norm, $\|O\|^2$. For the first term, $\frac{(\text{Tr}(O e^{-\beta H}))^2}{\text{Tr} e^{-2\beta H}}$, this can be proven as follows. Inserting the complete set of eigenstates $\{|\lambda\rangle\}$ of H , i.e., $H|\lambda\rangle = \lambda|\lambda\rangle$, we have

$$\begin{aligned} \frac{(\text{Tr}(O e^{-\beta H}))^2}{\text{Tr} e^{-2\beta H}} &= \frac{\sum_{\lambda, \tilde{\lambda}} \text{Tr}[O e^{-\beta H} |\lambda\rangle \langle \lambda| O e^{-\beta H} |\tilde{\lambda}\rangle \langle \tilde{\lambda}|]}{\text{Tr} e^{-2\beta H}} = \frac{\sum_{\lambda, \tilde{\lambda}} e^{-\beta \lambda} e^{-\beta \tilde{\lambda}} |\langle \lambda | O | \tilde{\lambda} \rangle|^2}{\text{Tr} e^{-2\beta H}} \\ &\leq \frac{1}{\text{Tr} e^{-2\beta H}} \sum_{\lambda, \tilde{\lambda}} \frac{e^{-2\beta \lambda} + e^{-2\beta \tilde{\lambda}}}{2} |\langle \lambda | O | \tilde{\lambda} \rangle|^2 = \text{Tr}[\rho_{2\beta} O^2] \leq \|O^2\| \leq \|O\|^2, \end{aligned} \quad (49)$$

where we have used the AM-GM inequality, $\sqrt{xy} \leq (x+y)/2$ for $x, y \in \mathbb{R}_{\geq 0}$.

We thus arrive at

$$\Pr[|\langle \psi_\beta | O | \psi_\beta \rangle - \text{Tr} \rho_\beta O| \geq \epsilon] \leq 4 \frac{\|O\|^2 \text{Tr} \rho_\beta^2}{\epsilon^2}, \quad (50)$$

which means that $|\psi_\beta\rangle$ satisfies Eq. (1) with $C_\epsilon = 4\|O\|^2/\epsilon^2$ and $e^{-\alpha n} = \text{Tr} \rho_\beta^2$. Note that the fact that $\text{Tr} \rho_\beta^2$ can be written as an exponential is explained in the main text.

PROOF OF THE MAIN RESULT: REQUIRED NUMBER OF SHADOWS FOR PREDICTING M THERMAL EXPECTATION VALUES

In this section we provide the detailed proof of Theorem 1 in the main text. We construct classical shadows of TPQ states (pure thermal shadows) by using two independent random unitaries. The first unitary, $U \sim \mathcal{Cl}(2^n)$, is followed by an application of $e^{-\beta H/2}$ to create a TPQ state, $|\psi_\beta\rangle$. The second unitary, V , combined with the measurement outcomes in the form of a bit string, $|b\rangle$, is used to construct the corresponding classical shadow, $\hat{\eta}_{V,b} = \mathcal{M}^{-1}(V^\dagger |b\rangle\langle b| V)$. We consider the cases where V is drawn from $\mathcal{Cl}(2^n)$, a random n -qubit Clifford measurement, and $\mathcal{Cl}(2)^{\otimes n}$, a random Pauli measurement, respectively. We start by deriving the mean-squared errors of the thermal shadows, Eqs. (8) and (9) in the main text, for both measurement protocols. Then, from a direct application of Theorem 2, we obtain Theorem 1 in the main text, which completes the proof.

Random Clifford measurements

The random Clifford measurement protocol consists of the application of a Clifford circuit $V \sim \mathcal{Cl}(2^n)$ to the TPQ state, $|\psi_\beta\rangle$, followed by a computational basis measurement with bit string outcome $|b\rangle$. We first compute the average, $\mathbb{E}[\text{Tr}\hat{\eta}_{V,b}O]$, and then the mean-squared error, σ^2 , with respect to the random Clifford measurement process. For the average we find,

$$\mathbb{E}[\text{Tr}\hat{\eta}_{V,b}O] = \mathbb{E}_U \mathbb{E}_{V,b}[\text{Tr}\hat{\eta}_{V,b}O] = \mathbb{E}_U[\text{Tr}\mathbb{E}_{V,b}[\hat{\eta}_{V,b}]O] = \mathbb{E}_U[\langle\psi_\beta|O|\psi_\beta\rangle] = \text{Tr}\rho_\beta O + \mathcal{O}(e^{-n}), \quad (51)$$

where we have used the fact that the averaged shadow reproduces the TPQ state, $\mathbb{E}_{V,b}[\hat{\eta}_{V,b}] = |\psi_\beta\rangle\langle\psi_\beta|$.

In order to compute the mean-squared error, we first write it in terms of the variance of the thermal shadow expectation value,

$$\sigma^2 = \mathbb{E}_U \mathbb{E}_{V,b}[(\text{Tr}\hat{\eta}_{V,b}O - \text{Tr}\rho_\beta O)^2] = \text{Var}[\text{Tr}\hat{\eta}_{V,b}O] + (\mathbb{E}_U \mathbb{E}_{V,b}[\text{Tr}\hat{\eta}_{V,b}O] - \text{Tr}\rho_\beta O)^2 = \text{Var}[\text{Tr}\hat{\eta}_{V,b}O] + \mathcal{O}(e^{-n}). \quad (52)$$

The thermal shadow variance can be computed from

$$\text{Var}[\text{Tr}\hat{\eta}_{V,b}O] = \mathbb{E}_U \mathbb{E}_{V,b}[(\text{Tr}\hat{\eta}_{V,b}O - \mathbb{E}_U \mathbb{E}_{V,b}[\text{Tr}\hat{\eta}_{V,b}O])^2] = \mathbb{E}_U \mathbb{E}_{V,b}[(\text{Tr}\hat{\eta}_{V,b}O_0)^2] - (\mathbb{E}_U \mathbb{E}_{V,b}[\text{Tr}\hat{\eta}_{V,b}O_0])^2, \quad (53)$$

where O_0 is the trace-less part of the observable O . Focusing on the first term, and invoking Eq. (31) for the random measurement process, we get

$$\mathbb{E}_U \mathbb{E}_{V,b}[(\text{Tr}\hat{\eta}_{V,b}O_0)^2] = \frac{2^n + 1}{2^n + 2} \mathbb{E}_U[\text{Tr}O_0^2 + 2\langle\psi_\beta|O_0^2|\psi_\beta\rangle] = \frac{2^n + 1}{2^n + 2} (\text{Tr}O_0^2 + 2\text{Tr}\rho_\beta O_0^2) + \mathcal{O}(e^{-n}). \quad (54)$$

From this we find that the variance is equal to

$$\text{Var}[\text{Tr}\hat{\eta}_{V,b}O] = \frac{2^n + 1}{2^n + 2} (\text{Tr}O_0^2 + 2\text{Tr}\rho_\beta O_0^2) - (\text{Tr}\rho_\beta O_0)^2 + \mathcal{O}(e^{-n}). \quad (55)$$

Combining this expression with Eq. (52) then results in Eq. (8) for the mean-squared error in the main text.

We note that the mean-squared error of the thermal shadows is, up to an exponential correction, equal to the σ^2 one obtains by plugging $\rho = \rho_\beta$ in Eq. (32). As such, for sufficiently large systems, shadows obtained from randomly measuring the TPQ state perform approximately as well as shadows obtained from measuring the true Gibbs state.

Random Pauli measurements

Random Pauli measurements can be performed by applying a tensor product of random single-qubit Clifford gates, $V = \bigotimes_{i=1}^n V_i$, to the TPQ state, $|\psi_\beta\rangle$, followed again by measurements in the computational basis with bit-string outcomes, $|b\rangle = \bigotimes_{i=1}^n |b_i\rangle$. For these random Pauli measurements, the quantum channel \mathcal{M} (Eq. (16)) is given by the depolarizing channel, $(D_{1/3})^{\otimes n}$, see e.g. Ref. [23] for the derivation. This means that the inverse channel is given by, $\mathcal{M}^{-1}(X) = (D_{1/3}^{-1})^{\otimes n}(X)$, and the classical shadow can be constructed from,

$$\hat{\eta}_{V,b} = \bigotimes_{i=1}^n D_{1/3}^{-1}(V_i^\dagger |b_i\rangle\langle b_i| V_i) = \bigotimes_{i=1}^n (3 V_i^\dagger |b_i\rangle\langle b_i| V_i - \mathbb{1}_i). \quad (56)$$

These shadows are just product states and hence can be stored and computed classically efficiently. From the definition of classical shadows (Eq. (17)), the shadows satisfy, $\mathbb{E}[\hat{\eta}_{V,b}] = |\psi_\beta\rangle\langle\psi_\beta|$. For this reason, the application of Eq. (51), results in the average

$$\mathbb{E}[\text{Tr}\hat{\eta}_{V,b}O] = \mathbb{E}_U\mathbb{E}_{V,b}[\text{Tr}\hat{\eta}_{V,b}O] = \text{Tr}\rho_\beta O + \mathcal{O}(e^{-n}), \quad (57)$$

for the expectation value of the Pauli shadows in Eq. (56). Thus, shadows from randomized Pauli measurements can, like Clifford measurements, be used as estimators for Gibbs state expectation values.

For the mean-squared error, we use Eq. (52) again and evaluate the first term in the variance (Eq. (53)) for the shadows constructed from Pauli measurements. For this we assume that we are interested in an observable O , which is a k -local Pauli operator, $O = P_1 \otimes \dots \otimes P_k \otimes I^{\otimes(n-k)}$. For more general observables our calculation below can be modified by using the results presented in the appendix of Ref. [23]. We find that the first term in the variance is given by,

$$\mathbb{E}_U\mathbb{E}_{V,b}[(\text{Tr}\hat{\eta}_{V,b}O)^2] = \mathbb{E}_U\mathbb{E}_V \sum_{b \in \{0,1\}^n} |\langle\psi_\beta|V|b\rangle|^2 \text{Tr}[O_0 (\mathcal{D}_{1/3}^{-1})^{\otimes n} (V^\dagger|b\rangle\langle b|V)]^2 \quad (58)$$

$$= \text{Tr}\left[|\psi_\beta\rangle\langle\psi_\beta| \bigotimes_{j=1}^k \mathbb{E}_{V_j} \sum_{b_j \in \{0,1\}} V_j^\dagger|b_j\rangle\langle b_j|V_j (3\langle b_j|V_j P_j V_j^\dagger|b_j\rangle)^2\right] = 3^k. \quad (59)$$

Here we have used the 2nd moment Haar integral [Eq. (22)] for a single qubit to compute the average over \mathbb{E}_{V_j} , and the fact that the contribution from $I^{\otimes(n-k)}$ evaluates to 1. Combining this with the second term in Eq. (53), and Eq. (52), leads to Eq. (9) in the main text.

Proof of Theorem 1

A direct application of Theorem 2 proves Theorem 1 presented in the main text. The median-of-means estimator of the Gibbs state expectation values, $\text{Tr}\rho_\beta O_j$, by the thermal shadows $\{\hat{\eta}_{V,b}\}$ is now defined as

$$\mu_j(N, K) = \text{median}[\mu_j^1(N), \mu_j^2(N), \dots, \mu_j^K(N)], \quad \mu_j^i(N) = \frac{1}{N} \sum_{\ell=N(i-1)+1}^{Ni} \text{Tr}\hat{\eta}_{V,b} O_j. \quad (60)$$

Then, Theorem 2 holds with σ_j^2 replaced by Eq. (52) for the mean-squared error of observable O_j . These errors are for random Clifford and Pauli measurements given by Eqs. (8) and (9) in the main text. This completes the proof of Theorem 1.

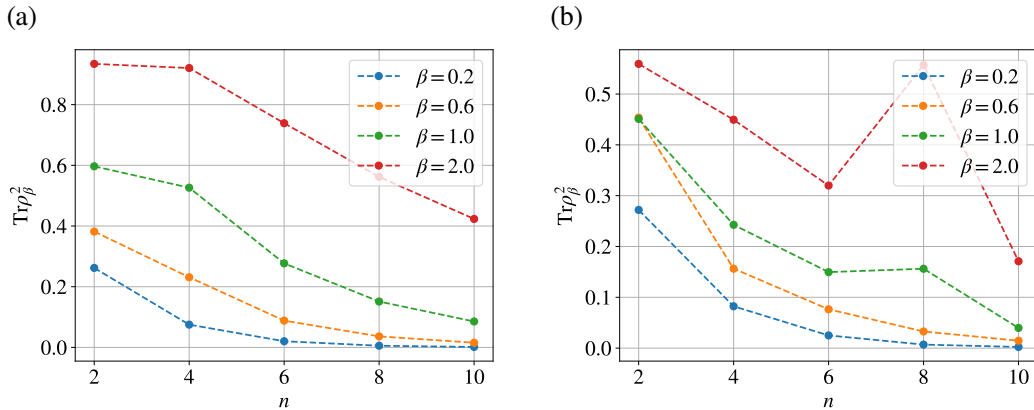


FIG. A1. Purity, $\text{Tr}\rho_\beta^2$, as a function of system size, n , for (a) the XXZ-Heisenberg model (with $J = 0.5$, $\Delta = 0.7$, and closed boundary conditions) and (b) a random Hamiltonian with all-to-all connectivity (the XYZ-Heisenberg model with random couplings between all qubits and a random field on each qubit). Note that for (b) we use a different random initialization for each n . The jump observed at $n = 8$ and $\beta = 2$ is an outlier.

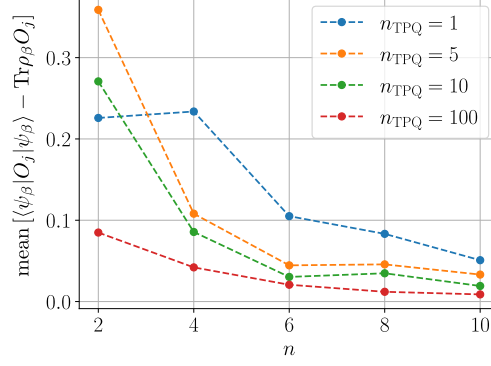


FIG. A2. Mean error of an ensemble of size $n_{\text{TPQ}} \in \{1, 5, 10, 100\}$ thermal pure states and different system sizes. For this we compute the mean error on all possible one- and two-qubit Pauli observables. We see that for larger n the required size of the ensemble, for a fixed mean error, becomes smaller in accordance with the vanishing of the variance. For these simulations, we used the XXZ-Heisenberg model with $J = 0.5$, $\Delta = 0.7$, and closed boundary conditions.

ADDITIONAL NUMERICAL EXPERIMENTS

In this section we present additional results obtained for some numerical experiments we ran, which support our claims in the main text. In Fig. A1, we show the purity, $\text{Tr} \rho_\beta^2$, of the Gibbs states for two different types of Hamiltonians as a function of the number of qubits, n . We observe that for both Hamiltonians the purity decreases (exponentially) with system size. The rate of decrease depends on the inverse temperature β . This is in accordance with our claim in the main text that, in general, the purity of the Gibbs state at finite temperature decreases with system size.

In Fig. A2, we show the mean error of the expectation values of all possible one-qubit Pauli operators and all two-qubit Pauli XX, YY and ZZ operators, $\{O_j\}$, in a batch of TPQ states, $\mathbb{E}_U [\langle \psi_\beta | O_j | \psi_\beta \rangle]$, as a function of system size. Note that here the average, \mathbb{E}_U , is taken over a total of n_{TPQ} TPQ states. When we increase the system size the mean error on all observables decreases for each different batch size, n_{TPQ} . This means that for large system sizes, $n \geq 10$, it might be possible to get away with only one single TPQ as the estimator for the Gibbs state.